Supporting Information

Mbughuni et al. 10.1073/pnas.1010015107

SI Materials and Methods

Reagents. Casamino acids low in salts and iron were purchased from Benton Dickinson, Inc. Yeast Extract was purchased from Biochemika Fluka. Sulfuric acid was purchased from Mallinckrodt. ^{57}Fe was purchased from Cambridge Isotopes at 95.5% purity. ^{57}Fe solution is prepared by dissolving 180 mg/mL ^{57}Fe in 9 M H_2SO_4. This solution is diluted 20% with diH_2O to a concentration of 9 mg/mL ^{57}Fe and 0.45 M H_2SO_4 for storage and use in growth media. Argon for preparing anaerobic samples was purchased from Praxair (≥99.99% pure, 6.0 research grade Ar). Trace contaminating O_2 was removed from the Argon gas by passage over an Agilent oxygen scrubber. Purchase of 4-nitrocatechol (4NC) was made from Sigma-Aldrich and recrystallized before use as previously described (1). All other chemicals were purchased from Sigma-Aldrich and used with no further purification.

Enzyme and Metal Quantification. Protein concentration was determined using absorbance at 280 nm (1.2 mg/mL/cm^{-1}) as previously described (2). Metal quantification was determined by Inductively Coupled Plasma–Optical Emission Spectroscopy (ICP–OES) using a Thermo Scientific iCAP 6500 dual view ICP–OES. ^{57}Fe concentrations were estimated via Mössbauer spectroscopy. ICP-OES samples are prepared by release of the iron with 18% nitric acid following removal of the precipitated enzyme by centrifugation. Homoprotocatechuate 2,3-dioxygenase (2,3-HPCD) was routinely purified with iron occupancy of 85–95%; the main contaminant is Mn at <7% occupancy. ^{57}Fe occupancy was determined to be 80–95% by comparing protein concentrations to Mössbauer quantifications for the total iron in ^{57}Fe-enriched 2,3-HPCD from several different 2,3-HPCD preparations.

Spectroscopy. EPR spectra were collected using a Bruker Elexsys E-500 or Bruker ESP 300 spectrometers equipped with Bruker dual mode cavities and Oxford ESR 910 liquid helium cryostats. Spectra were analyzed using the software package SpinCount (M.P. Hendrich, Carnegie Mellon University). Signal quantification was relative to a Cu^{II}EDTA or Fe^{III}EDTA spin standard using SpinCount. Absorption spectra were collected using an Applied Photophysics model SX.18 MV stopped-flow spectrometer fitted with a diode array detector or a Hewlett-Packard 8453 diode array spectrophotometer. Mössbauer spectroscopy was performed as previously described (3). Spectra were analyzed using the software WMOSS (SEE Co.).

Density Functional Theory (DFT) Calculation. The DFT calculations were performed with Gaussian '03 (Revision E.01) (4) using the hybrid functional B3LYP and basis set 6-311G. The computational structure includes the iron and its ligands (dioxygen, 4NC, Glu267, His155, and His214) and second coordination sphere residues (Asn157, Trp192, Asn200, and Tyr257). The atom positions of the dioxygen and the 4NC were optimized; the remaining atoms were positioned on the basis of the wild type 2,3-HPCD-4NC structure (PDB ID code 2IGA, subunit C). Residue His200 was changed to Asn and optimized using COOT (5). A planar 4NC aromatic ring and end-on bound dioxygen were modeled as the starting point for computations.

SI Results

Int-1 Structure from DFT Calculations. The DFT optimizations were performed for states with spins $S = 2$ and $S = 3$. The calculation for the $S = 3$ state resulted in a Fe^{III}-$O_2^{\bullet-}$ state in which the spin of the Fe^{III} ($S_{Fe} = 5/2$) is parallel to the spin of the $O_2^{\bullet-}$ ($S_{sox} = 1/2$) moiety. [Note that this calculation did *not* converge to the plausible alternative state, namely, the Fe^{II}-O_2 state in which the spins of Fe^{II} ($S_{Fe} = 2$) and O_2 ($S_{ox} = 1$) are parallel and yield total spin $S = 3$.] Based on the ferromagnetic solution, we prepared a guess state to initiate the calculation for the broken symmetry state that mimics the spin two state obtained by coupling the spin of the $O_2^{\bullet-}$ ($S_{sox} = 1/2$) antiparallel to the spin of Fe^{III} ($S_{Fe} = 5/2$). The difference between the energies for the ferromagnetic state and the broken-symmetry state implies a ferromagnetic coupling constant J of −5.8 cm^{-1} ($J\mathbf{S}_{Fe}\cdot\mathbf{S}_{sox}$ convention). This value and those for selected hyperfine parameters are listed in Table S1 together with the corresponding experimental values. The structure for the broken-symmetry state, which closely matches the structure for the ferromagnetic state, is shown in Fig. S6*A*. Using the perspective of Fig. S6*A*, Fig. S6*B* depicts the spin density profile for the broken-symmetry state. The shape of the π^* orbital containing the radical electron is clearly recognizable from the contour plot. Table S2 lists the spin populations for iron and the oxygen atoms of the superoxo ligand in the broken-symmetry state and the ferromagnetic state. The spin populations indicate that the superoxo bond is somewhat polarized by the iron. Using the averages over the two spin states, we obtain different spin populations for oxygens: $(0.29 + 0.48)/2 = 0.385$ for the proximal oxygen and $(0.59 + 0.64)/2 = 0.615$ for the distal oxygen (the difference can be seen from the spin density plot in Fig. S6*B*). The averaged spin populations for the two oxygens add up to a total of 1.000, representing the radical electron. The spin population of the iron is smaller than the number of five for a free high-spin Fe^{III}, indicating some degree of spin density transfer to the ligands. The spin populations for the oxygen atoms in Table S2 can be decomposed as $-0.385 + 0.095 = -0.29$ (O_{prox}) and $-0.615 + 0.025 = -0.59$ (O_{dist}) for the broken-symmetry state and $0.385 + 0.095 = 0.48$ (O_{prox}) and $0.615 + 0.025 = 0.64$ (O_{dist}) for the ferromagnetic state. The quantities +0.095 and +0.025 are the contributions to the spin populations arising from spin polarization of the superoxo by the high-spin Fe^{III} site, which are positive in both the ferromagnetic and broken-symmetry states and yield a total of spin transfer 0.12 from iron to superoxo. The differences in the spin densities for the proximal and distal oxygen are reflected in the magnetic hyperfine parameters listed in Table S1.

1. Groce SL, Miller-Rodeberg MA, Lipscomb JD (2004) Single-turnover kinetics of homoprotocatechuate 2,3-dioxygenase. *Biochemistry* 43:15141–15153.
2. Miller MA, Lipscomb JD (1996) Homoprotocatechate 2,3-dioxygenase from *Brevibacterium fuscum*—A dioxygenase with catalase activity. *J Biol Chem* 271:5524–5535.
3. Fox BG, Shanklin J, Somerville C, Münck E (1993) Stearoyl-acyl carrier protein Δ^9 desaturase from *Ricinus communis* is a diiron-oxo protein. *Proc Natl Acad Sci USA* 90:2486–2490.
4. Frisch MJ, et al. (2004) *Gaussian 98* (Gaussian, Wallingford, CT).
5. Emsley P, Cowtan K (2004) Coot: Model-building tools for molecular graphics. *Acta Crystallogr* E60:2126–2132.
6. Chiesa M, et al. (2002) Continuous wave electron paramagnetic resonance investigation of the hyperfine structure of $^{17}O_2$- adsorbed on the MgO surface. *J Chem Phys* 116:4266–4274.

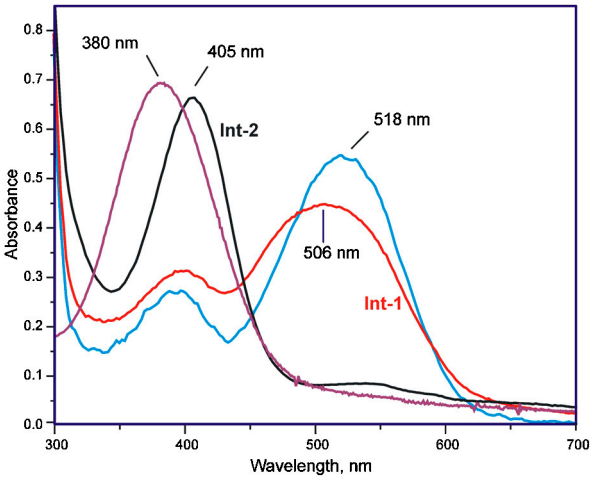

Fig. S1. Absorption spectra (path length 0.2 cm). Blue: The anaerobic H200N-4NC complex. Red: Int-1, 10 s after mixing H200N-4NC complex with O_2 saturated buffer at 4 °C. Black: Int-2, 10 min after mixing. Maroon: Released product purified from the end complex. The product was isolated using a G25 PD10 column after denaturing the enzyme with 7 M urea. The relative absorbance of the isolated product is approximate on this figure. Reaction conditions prior to mixing: 400 μM H200N-4NC, 200 mM MOPS buffer, pH 7.5.

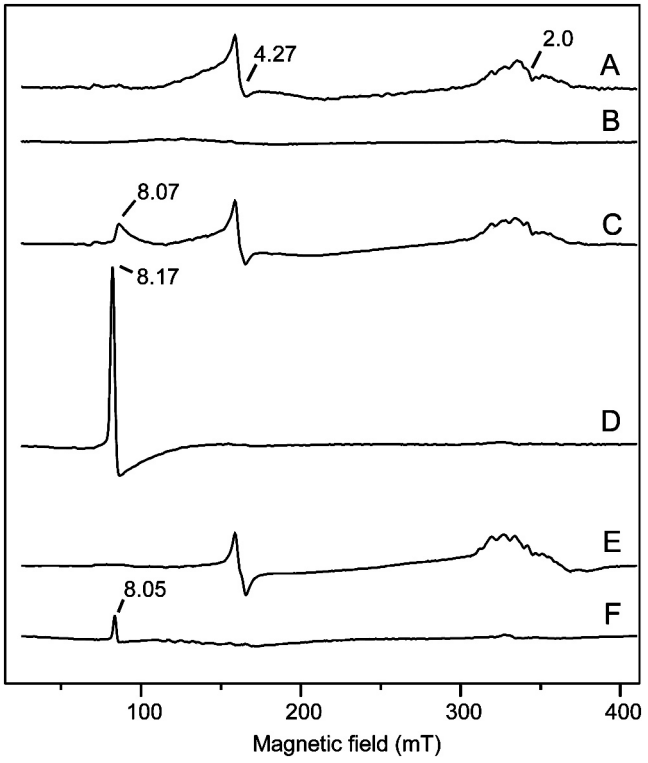

Fig. S2. EPR spectra of reaction intermediates. Anaerobic H200N-4NC complex, (*A*) perpendicular mode spectra and (*B*) parallel mode spectra; 10 s after mixing H200N-4NC complex with O_2 at 4 °C, (*C*) perpendicular mode spectra and (*D*) parallel mode spectra; End complex, (*E*) perpendicular mode spectra and (*F*) parallel mode spectra. Conditions prior to mixing: 1.64 mM H200N-4NC, 200 mM MOPS buffer pH 7.5. EPR measurement conditions: Frequency, 9.65 GHz (*A*, *C*, and *E*) or 9.35 GHz (all others); microwave power, 4 mW; temperature, 2 K; and modulation amplitude, 10 G. The *g* values of resonances are marked on the figure.

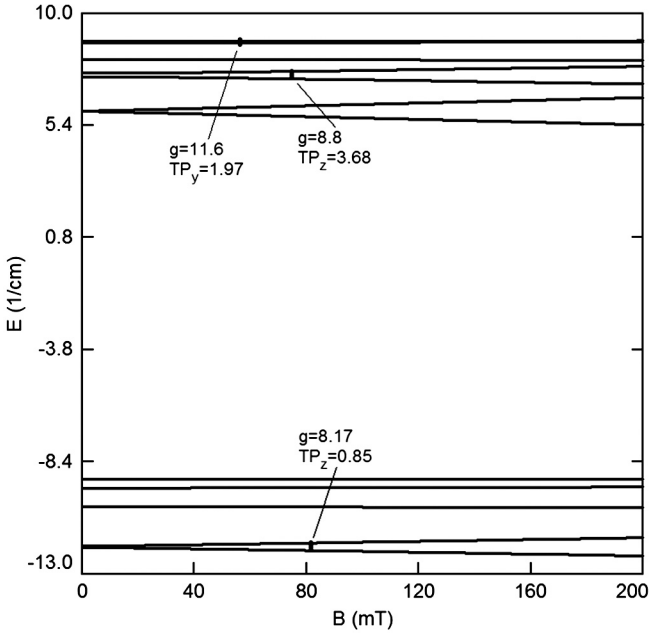

Fig. S3. Energy level diagram for the spin system of Int-1; approximate $S = 2$ ground and $S = 3$ excited multiplets. The parameters used are the same as those cited in Fig. 1 of the main text. Energy splittings are shown as a function of the applied magnetic field, B. The $g = 8.17$ and 8.8 transitions are observed with B along z, whereas the $g = 11.6$ resonance is observed along y. Relative transition probabilities (TP) are given.

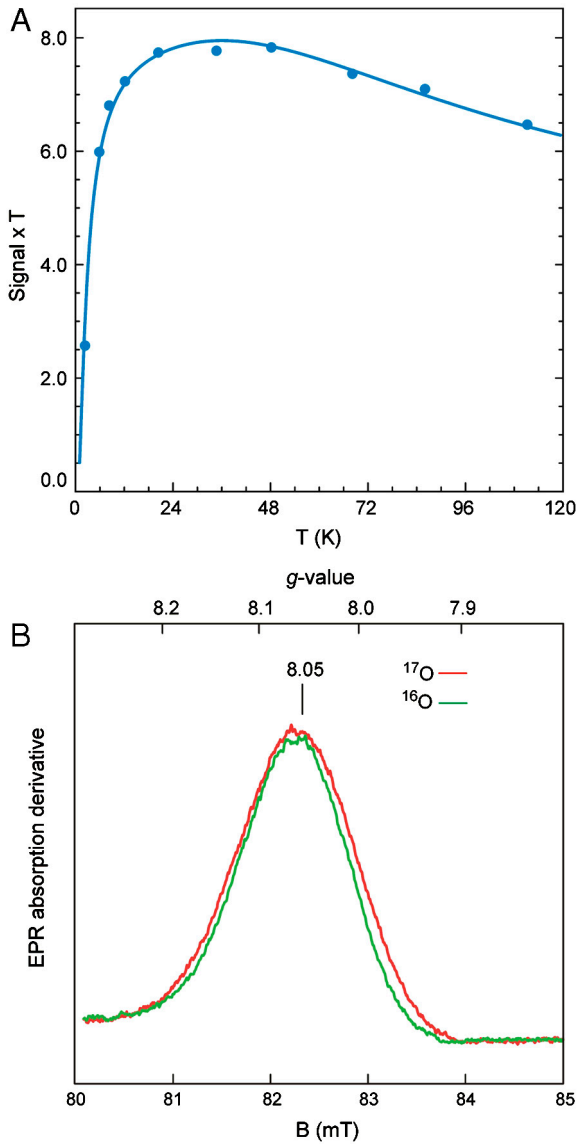

Fig. S4. (*A*) Signal × temperature versus temperature of the $g = 8.05$ parallel mode EPR signal of Int-2 (dots) recorded with nonsaturating microwave powers. The fit (line) uses the parameters given in Table 1 of the main text. (*B*) ^{17}O-hyperfine broadening of Int-2. Parallel mode EPR spectra of the $g = 8$ region for samples frozen 10 min after mixing with ~1 eq of $^{16}O_2$ or 70% $^{17}O_2$. Conditions before mixing with O_2 saturated buffer at 4 °C: 1.7 mM H200N-4NC, 200 mM MOPS pH 7.5. EPR conditions: frequency, 9.28 GHz; power, 20 mW; modulation, 10 G; and temperature, 5 K.

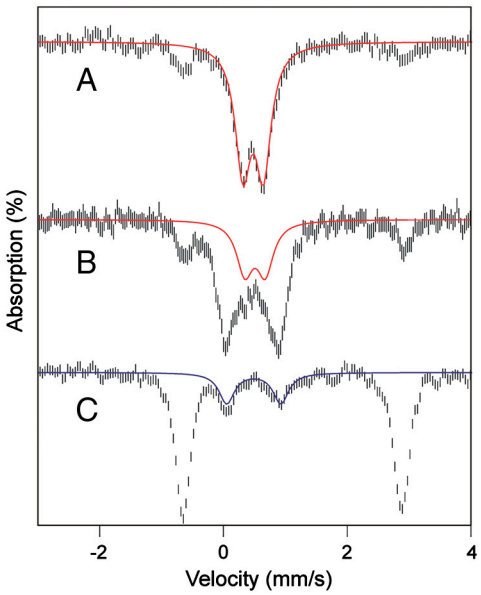

Fig. S5. Mössbauer spectra recorded at 4.2 K for $B = 0$ of the single turnover time course in the presence of 2 × 4NC at 4 °C. (*A*) 24 ms after mixing 1 eq H200N–2 eq 4NC complex with 1 eq of O_2. The sample at this time point is prepared by freezing the reaction mixture on counterrotating aluminum wheels at Liq N_2 temperatures. The red line is a fit to the data using the parameters from Table 1. (*B*) Eighty seconds after mixing with O_2. This sample is prepared by shooting the reaction mixture into an anaerobic vial for aging before freezing the sample in Liq N_2. The red line shows the contribution of Int-1 to the spectrum. (*C*) The end complex. This sample is a rapid freeze quench powder frozen in Liq N_2, transferred into the anaerobic glovebox, then thawed for 20 min at 25 °C. The blue line shows the contribution of Int-2 to the spectrum. Concentrations before mixing: 1.62 mM H200N-4NC (plus one additional equivalent of 4NC), 200 mM MOPS pH 7.5.

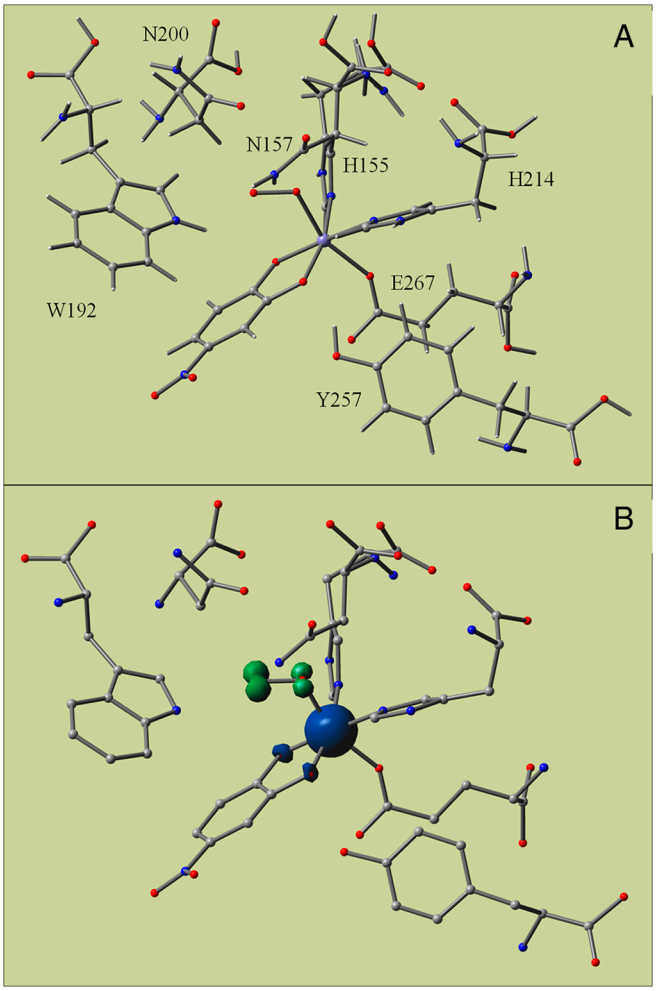

Fig. S6. (*A*) Structure of the truncated model for Int-1 adopted in DFT calculations. (*B*) Spin density contour plot for broken symmetry state of Int-1 obtained with DFT. Majority spin (centered at iron) is in blue and minority spin (at superoxo) is in green.

Table S1. Hyperfine parameters and exchange coupling constants for Int-1 From experiment and DFT

	^{57}Fe			^{17}O superoxo	
	δ, mm/s	ΔE_Q, mm/s	J, cm^{-1}	$A_{proximal}$, MHz	A_{distal}, MHz
Experiment	0.50	−0.33	6	—*	180†, —*, —*
DFT	0.56	−0.66	−5.8	−123, +74, +128‡	−226, +59, +81‡
Ref. (6)				−214, +20, +23‡	

*Not measured.
†Experimental 180 MHz splitting is assumed to be associated with the distal oxygen atom.
‡Values for $A_{x'}$, $A_{y'}$, and $A_{z'}$. z is along O–O bond, x in plane of π* orbital.

Table S2. Mulliken spin populations

	Broken symmetry state	Ferromagnetic state
Fe	4.25	4.24
$O_{proximal}$	−0.29	0.48
O_{distal}	−0.59	0.64